Multiobjective Optimal Placement of Convectively Cooled Electronic Components on Printed Wiring Boards

Nestor V. Queipo, Joseph A. C. Humphrey, and Alfonso Ortega, *Member, IEEE*

***Abstract*— This paper presents a solution methodology for multiobjective optimization problems in the context of models for the placement of components on printed wiring boards (PWB's). The methodology combines the use of a flow and heat transfer solver, a genetic algorithm for the adaptive search of optimal or near-optimal solutions, and a multiobjective optimization strategy [Pareto optimization or multiattribute utility analysis (MUA)]. Using as the optimization criterion the minimization of an estimate of the failure rate of the system of components due to thermal overheating (via an Arrhenius relation), the effectiveness of the present solution methodology is demonstrated by reference to a case with *known* optimal solutions. The results obtained using the same solution methodology for a multiobjective optimization problem (a variation of the case study) involving the minimization of the aforementioned total failure rate of the system as well as the minimization of the total wiring length (given some interconnectivity requirements) are presented and discussed for both Pareto optimization and MUA.**

***Index Terms*— Electronics cooling, genetic algorithms, multiobjective optimal placement, printed wiring boards, thermal management.**

I. Introduction

THE optimal placement of components on printed wiring boards requires satisfying multiple, possibly conflicting, design objectives. As pointed out by Moresco [1], these design objectives may be very different in nature—geometrical, electrical, thermal, mechanical, and cost (manufacturing and maintenance)—which makes finding the "best" design a complicated task.

Two major design objectives are related to the reliability (thermal/mechanical/cost) and the routing (electrical/cost) requirements of the component placement design. Specifically, the minimization of estimates of the *failure rate* of the system and *total wiring length* are design objectives of prominent interest. The former optimization criterion imposes major heat transfer requirements on the design because of the combined effects of:

1) rapidly increasing packaging density and power dissipation demands;
2) potentially high costs associated with the failure of electronic components, as pointed out by Weiss *et al.* [2] and Wessely *et al.* [3] among others.

The latter is critical because of electrical performance, speed, and transmission line requirements and its impact on the manufacturing costs.

Most optimization studies regarding component placement have considered a single design objective, such as reliability (see, for example, [4]–[6]), or routing (see, for example, [7], [8], and many others reported in [9]). With the exception of the work by Osterman *et al.* [10], the few optimization studies that have addressed multiple objectives have failed to provide rigorous methods to select the "best" design [11] or have made somewhat arbitrary choices regarding the relative importance of the design objectives under consideration [12]–[14]. The solution methodology proposed by Osterman *et al.* [10] includes a thermal resistive network approach for predicting the temperatures in the heated elements, an optimization strategy based on the force-directed placement methodology and the weighting method for combining the various optimization objectives.

This study overcomes some of the limitations of previous studies in this area and discusses a methodology to select the "best" component placement design when multiple design objectives are present. The methodology is based on the concepts of Pareto optimality [15] and multiattribute utility analysis (MUA) [16]. The Pareto optimization provides a set of alternative component placements from which the "best" design must be selected, and the MUA assists in the process of articulating the designer's preferences and identifying the "best" component placement (decision problem). As reported by Thurston [17], the MUA has been successfully applied to a wide variety of decision problems, including trajectory selection for NASA missions, nuclear power plant site selection, telecommunication system architecture design, and many others.

The remainder of this paper is structured as follows. Section II provides a formal definition of the problem of interest and Section III gives a description of the different elements of the present solution methodology and their

Manuscript received June 1, 1996; revised December 1, 1997. This work was supported in part by the Fundación Gran Mariscal de Ayacucho, the Universidad del Zulia, and the Consejo Nacional de Investigaciones Científicas y Tecnológicas, Venezuela. This paper was recommended for publication by Associate Editor C. H. Amon upon evaluation of the reviewers' comments.

N. V. Queipo is with the Instituto de Cálculo Aplicado, Facultad de Ingeniería, Universidad del Zulia, Zulia 4005, Venezuela.

J. A. C. Humphrey is with the College of Engineering, Bucknell University, Lewisburg, PA 17837 USA.

A. Ortega is with the Department of Aerospace and Mechanical Engineering, University of Arizona, Tucson, AZ 85721 USA.

Publisher Item Identifier S 1070-9886(98)02219-7.

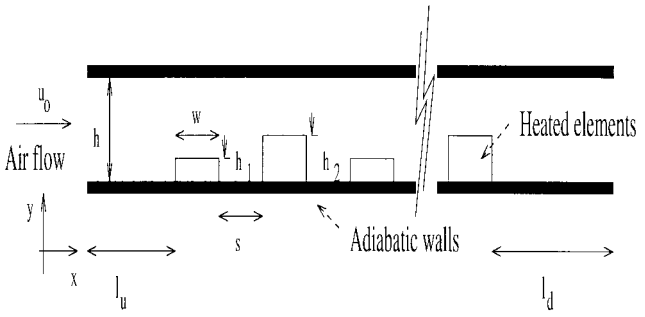

Fig. 1. Schematic of the heat transfer configuration of interest.

interaction. In particular, Section III describes a flow and heat transfer solver, a genetic algorithm and two different multiobjective optimization strategies (Pareto optimization and MUA). A description of a case study designed to validate and evaluate the present solution methodology is the subject of Section IV. The paper ends with the application of the present solution methodology to a multiobjective optimization problem (a variation of the case study) using both Pareto optimization and MUA.

II. Problem Definition

The problem of interest here corresponds to the optimal placement of convectively cooled electronic components on printed wiring boards (PWB) subject to *thermal* and *nonthermal* optimization criteria. Because of its cost effectiveness and mechanical simplicity, forced air cooling is the most frequently used technique for cooling electronic components in personal computers and work stations. These systems comprise a major portion of the market with moderate heat transfer rate requirements. The convectively cooled electronic components on printed wiring boards are modeled here as equally spaced heated elements placed on the bottom wall of a ventilated two-dimensional (2-D) channel, as illustrated in Fig. 1. The printed wiring board is aligned parallel to the coolant flow which is assumed laminar and 2-D. Each component is assumed to dissipate a constant heat flux and the heat fluxes may differ among components.

Regarding thermal optimization, forced air cooling is usually limited by acoustic noise constraints placed on the fan driving the flow, and arrangements of electronic components that maximize reliability and minimize thermo-mechanically induced stresses are highly desirable. Examples of nonthermal optimization criteria include the need to minimize the total wire length on the PWB, clustering functionally related components to conform to speed and transmission line requirements, and keeping analog components and digital components separate to reduce crosstalk.

In this study, the minimization of the failure rate of the electronic components on the printed wiring boards due to thermal overheating, and the minimization of the total wiring length satisfying the requirements specified by an interconnectivity matrix, are selected as *thermal* and *nonthermal* optimization criteria, respectively.

The reliability prediction is the statistical estimate of the value of time over which a device will function. The inverse

	1	2	3	4	5
1	1	1	1	0	0
2	1	1	0	1	0
3	1	1	1	0	0
4	0	1	0	1	0
5	0	0	0	0	1

Fig. 2. Example of an interconnectivity matrix for five components. A unit entry indicates a pair of components that are "functionally related" while a zero entry indicates a pair of components that are "not functionally related."

of the reliability of a device is called its *failure rate* and is measured in failures per megahours (fr Mh^{-1}). As indicated by, for example, Moresco *et al.* [1], and Wessely *et al.* [3], the failure rate of an electronic component is a strong function of its temperature.

Even though various functional relationships between failure rate and temperature in electronic components have been suggested (Wong [18]), according to Blanks [19], the Arrhenius relation is the most widespread model among practitioners in the electronic packaging industry. In this study, the failure rate of electronic component "i" is estimated using the Arrhenius relation as

$$\lambda_i = A_i \exp(-B_i/T_i^{\max}). \tag{1}$$

Here A_i and B_i are constants associated with the thermal sensitivity of the electronic component, while $T_i^{\max}$ is the maximum temperature of component "i." Of interest here is the general case for which the electronic components on the PWB may differ in heat dissipation rate and thermal sensitivity. Since the failure rate of a component depends strongly on temperature as specified by (1), the maximum temperature of each component is calculated by solving numerically the conservation equations for continuity, momentum, and energy.

One of the objective functions to be minimized in this study is the total failure rate of a system consisting of a number of electronic components equal to N_{com} and given by the sum of the individual component failure rates as shown in

$$\lambda_{\text{total}} = \sum_{i}^{N_{com}} \lambda_i. \tag{2}$$

The wiring requirements among different components is represented by an interconnectivity matrix (I). An entry I_{ij} in the interconnectivity matrix (see Fig. 2) is given the value 1 if component "i" is functionally related to component "j" or the value 0 otherwise.

If we denote the wiring length between components "i" and "j" by the variable L_{ij}, the additional objective function to be

satisfied is the minimization of

$$g = \sum_{i=1}^{N_{comp}} \sum_{j=1}^{i} L_{ij} \cdot I_{ij}. \tag{3}$$

In summary, the problem of interest may be stated as follows: given N_{com} heated elements to be distributed among N_{com} equally-spaced locations on the bottom wall of a 2-D ventilated channel, what are some of the arrangements that minimize both a measure of the failure rate of the system and the total wiring length required to meet the wiring requirements associated with a given interconnectivity matrix?

III. Solution Methodology

The solution methodology, illustrated in Fig. 3, has three elements: a flow and heat transfer solver, a genetic algorithm, and a multiobjective optimization strategy. The flow and heat transfer solver is responsible for the accurate prediction of the maximum temperature of each heated element used for calculating the individual failure rates. The multiobjective optimization strategy provides the means to convert the original multiobjective optimization problem into a form amenable to be solved by the genetic algorithm. The genetic algorithm is responsible for the adaptive search of optimal or near-optimal solutions. Note that even for the simplified model formulated in this study the thermal optimal placement of electronic components with different heat generation rates and thermal sensitivities would require an exhaustive investigation of the entire solution space which, in this case, is combinatorial. For example, if eight different components are considered, the number of possible arrangements is 40 320 (8!) and, as indicated by De Jong [20], nonadaptive search procedures may be computationally prohibitive. Specifically, for the case of interest, the time needed to compute the maximum heated element temperatures for any given arrangement (see next section) on a workstation (IBM RISC 6000/530) was approximately 30 min, and as result, it would take about 2.3 years to exhaustively investigate the solution space.

A. Flow and Heat Transfer Solver

For the purpose of estimating the failure rate of a given arrangement of electronic components on a printed wiring board using the model adopted in this investigation, it is necessary to estimate the maximum temperature on the surface of each heated element. This temperature is a function of the air velocity field, the thermal boundary conditions exhibited by the heated elements, the specific geometry (size and height of the heated elements), distance between heated elements, substrate conduction characteristics, and the distance from the inflow boundary to the first heated element. If the substrate is assumed to be adiabatic, and the heat fluxes on the element surfaces are specified, the maximum surface temperature of each heated element can be obtained by solving the conservation equations of mass, momentum and energy in the fluid subject to appropriate boundary conditions. Note that the selected boundary conditions for the heated elements and the substrate are a compromise solution between computational effort and modeling accuracy. While modeling the electronic components on a printed wiring board as heat generating blocks on a conductive substrate would have been more accurate, it would have made the numerical simulations unnecessarily longer for the purpose of this work.

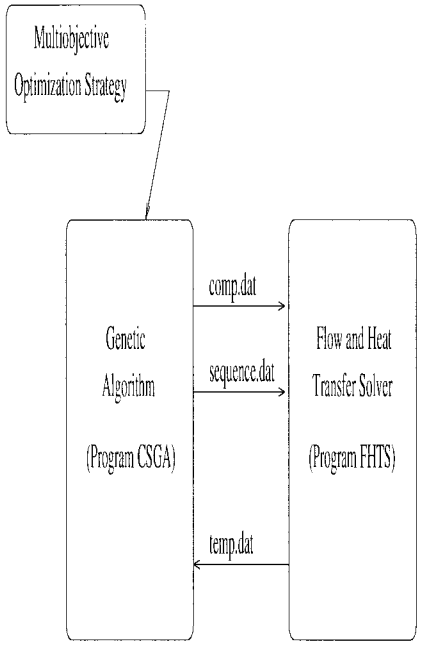

Fig. 3. Illustration of the solution methodology.

Steady state results for the velocity and temperature fields can be obtained by either solving the unsteady form of the conservation equations and marching in time or by solving the steady state form of the conservation equations in an iterative framework using under-relaxation. Jang *et al.* [21] show that the latter approach may be more efficient in terms of CPU time required to achieve steady state results and it is the approach adopted in this investigation.

Assuming steady, 2-D laminar fluid flow with constant physical properties, and neglecting natural convection (this assumption is justified later) and viscous dissipation effects, the nondimensional conservation equations for mass, momentum and energy in the fluid phase are given by (4)–(7), respectively:

$$\frac{\partial U}{\partial X} + \frac{\partial V}{\partial Y} = 0 \tag{4}$$

$$\frac{\partial UU}{\partial X} + \frac{\partial VU}{\partial Y} = -\frac{\partial P}{\partial X} + \frac{1}{Re}\left\{\frac{\partial^2 U}{\partial X^2} + \frac{\partial^2 U}{\partial Y^2}\right\} \tag{5}$$

$$\frac{\partial UV}{\partial X} + \frac{\partial VV}{\partial Y} = -\frac{\partial P}{\partial Y} + \frac{1}{Re}\left\{\frac{\partial^2 V}{\partial X^2} + \frac{\partial^2 V}{\partial Y^2}\right\} \tag{6}$$

$$\frac{\partial U\theta}{\partial X} + \frac{\partial V\theta}{\partial Y} = \frac{1}{Re\ \mathrm{Pr}}\left\{\frac{\partial^2 \theta}{\partial X^2} + \frac{\partial^2 \theta}{\partial Y^2}\right\}. \tag{7}$$

The dimensionless quantities appearing in these equations are

$$X = \frac{x}{h},\ Y = \frac{y}{h},\ U = \frac{u}{u_o},\ V = \frac{v}{u_o}$$
$$P = \frac{p}{\rho u_o^2},\ \theta = \frac{T - T_o}{q_r'' h/k},\ Re = \frac{u_o h}{\nu},\ \mathrm{Pr} = \frac{\nu}{\alpha}.$$

TABLE I
NON-DIMENSIONAL AND GEOMETRIC PARAMETER VALUES USED IN THIS WORK

Parameter	Re	Pr	h_1/h	h_2/h	s/h	w/h	l_u/h
Value	750.0	0.7	0.1	0.2	0.5	0.5	3.0

In these expressions, the symbols α and ν denote thermal diffusivity and kinematic viscosity, respectively. The symbol q_r'' represents the total heat flux provided by any one of the heated elements taken as a reference value.

For the channel flow considered in this investigation (see Fig. 1) uniform velocity and temperature distributions are imposed at the inlet. Except for the inflow boundary, all exposed channel surfaces are taken as adiabatic. In general, selecting accurate boundary conditions at open boundaries has been shown to be difficult [22]. In this study, the streamwise velocity and temperature gradients are assumed to be zero at the outlet. Blosh *et al.* [23] have shown that the specification of velocity gradients equal to zero is a good boundary condition for the open boundary of channel flow configurations, provided the velocity at the outlet is corrected so that global conservation of mass is enforced. The temperature gradient equal to zero (thermally fully developed flow) is imposed at a distance sufficiently removed from the last heated element so that the computed maximum temperature of each heated element is unaffected.

The boundary conditions are as follows:

Inlet plane	$U = 1.0$, $V = 0$, $\theta = 0$;
Outlet plane	$\partial U/\partial X = 0$, $\partial V/\partial X = 0$, $\partial\theta/\partial X = 0$, and $\int_{0.0}^{1.0} U dY = 1$;
Top and bottom walls	$U = V = 0$;
Top and bottom walls	$\partial\theta/\partial Y = 0$;
Heated elements	$U = V = 0$, $\partial\theta/\partial n\|_s = q''/q_r''$.

The initial condition imposed on the flow field calculations corresponded to developed flow in a channel at every streamwise location except within the solid heated elements where velocities were set to zero. The initial temperature field in the fluid was set equal to the inlet temperature.

The configuration geometry is specified by the number of heated elements, the channel height (h), the heated element width (w), heated elements height (h_1, h_2), the inter-element spacing (s), the distance from the inlet plane to the first element (l_u) and the distance from the last element to the exit plane (l_d) (see Fig. 1).

The nondimensional values adopted for these quantities are summarized in Table I and are close to the values reported by Kim [24] as typical of models of electronic components on printed wiring boards. The value of the geometrical parameter l_d/h is selected such that the location of the exit plane does not significantly affect the maximum temperatures calculated on the surfaces of the heated elements. As in Queipo *et al.* [12], the number of heated elements considered is eight.

In this study, the cooling fluid is air and all physical properties are evaluated for air at 300 K. The channel height was assumed to be 0.02 m and the inlet velocity $u_o = 0.59$ m/s, corresponding to a Reynolds number of $Re = 750$. The Prandtl number of air at the reference temperature was taken as $\mathrm{Pr} = 0.7$.

The program flow and heat transfer solver (FHTS) was used to perform the numerical calculations of flow and heat transfer. The program finds its origins in the ROTFLO2 program developed by Hayase *et al.* [25] and allows the direct numerical simulation of unsteady, three-dimensional, nonisothermal, constant property laminar flow in Cartesian or cylindrical coordinates. The numerical procedure solves for the primitive variables (velocity and pressure) and is based on the finite difference equations derived using the staggered grid control-volume formulation presented by Patankar [26], but with the convective coefficients discretized using the QUICK scheme as suggested by Hayase *et al.* [27]. FHTS includes the codification of a variety of velocity-pressure coupling algorithms such as the SIMPLE procedure of Patankar and Spalding [28], the SIMPLER procedure of Patankar [26], and the SIMPLEC procedure of VanDoormaal *et al.* [29]. The program FHTS has been described and successfully tested in Queipo [14] using a variety of standard flow and heat transfer benchmark test cases. These include the cavity driven flow of Ghia *et al.* [30], and the backward facing step flow and heat transfer of Gartling [31] and Runchal [32], among others.

The velocity field for each configuration is calculated using the SIMPLE algorithm with an under-relaxation factor for the velocities $\alpha = 0.7$. The under-relaxation factor for pressure was taken as 1-α. According to Peric [34] (see Dainese [33]) this relation between the velocity and pressure under-relaxation factors is optimal. Convergence was achieved when a variable (ϵ) representing the maximum mass, U-momentum and V momentum residual fell below a given predefined value. These residuals are computed as the sum of the absolute values of the corresponding mass or momentum imbalances over each of the control volumes in the domain. A convergence criteria of $\epsilon \leq 10^{-4}$ was used for computing the velocity field.

The temperature field is obtained using an under-relaxation parameter equal to 0.9. Convergence in the numerical calculation of temperature was achieved when a variable ϵ representing the energy residual fell below a given predefined value. This residual is computed as the sum of the absolute value of the energy imbalance of each of the control volumes in the domain. A convergence criteria of $\epsilon \leq 10^{-5}$ was used to compute the temperature field.

B. Genetic Algorithm

Genetic algorithms are adaptive search procedures loosely based on the Darwinian notion of evolution that have been employed successfully in a variety of search, optimization and machine learning applications. The genetic algorithm in this study corresponds to the Combinatorial Simple Genetic Algorithm encoded in the program CSGA, documented in Queipo [14]. The CSGA program has the structure of the program GAucsd (v. 1.4) developed by Schraudolph *et al.* [35], but uses a different representation (integer representation) and different recombination operators (partially matched crossover). In addition, the random number generator in the program CSGA is the routine RAN2 available in *Numerical*

Recipes by Press *et al.* [36]. For a general introduction to genetic algorithms, see [37] or [38]. An introduction to genetic algorithms in the context of thermosciences applications is given by Queipo *et al.* [13].

The interaction between the flow and heat transfer solver and the genetic algorithm is illustrated in Fig. 3. There are two key elements to consider in describing the connection between CSGA and FHTS:

1) the control structure of their coupled execution;
2) the information exchange between the two programs.

During the coupled execution of the CSGA and the FHTS programs, CSGA is the master process and FHTS is the slave process. Each time the program CSGA requires the evaluation of a new candidate solution, a slave process is created and the execution of CSGA is suspended. Within the slave process, the program FHTS is invoked and after its successful completion, CSGA resumes its execution. All this is done within a UNIX operating system environment.

The CSGA and the FHTS programs exchange information through data files. The program CSGA makes available to FHTS two files:

1) a file called *comp.dat* describing the geometrical and thermal characteristics of the heated elements in the candidate solution;
2) a file called *sequence.dat* describing the order in which the heated elements specified in *components.dat* are positioned along the bottom wall of the ventilated channel.

The program FHTS generates the file *temp.dat* after its successful execution. The file *temp.dat* contains the maximum temperature on the surface of each of the heated elements in the candidate solution.

C. Multiobjective Optimization

In contrast to the optimization of a single function where the term optimum value has a unique meaning and geometric interpretation, in the case of multiobjective optimization there is not a general definition of the optimal values. Here, the term optimization means to find a solution that provides acceptable values for the objective functions and that satisfies the preference structure of the person posing the problem; that is, the designer.

Hence, the problem in multiobjective optimization consists in finding a vector of design variables that satisfies a set of constraints and that optimizes a second vector whose elements represent the objective functions. There is no single best approach for solving these problems. Different philosophies and methodologies co-exist for addressing optimization problems with multiple objectives. The approaches differ in their view concerning whether or not it is possible (or practical) to capture the preference structure of the designer. The spectrum of methods begins with Pareto optimization where there is no information regarding the preference structure of the designer, and ends with the MUA (Keeney *et al.* [16]) where it is assumed possible to capture the aforementioned preference structure.

1) Pareto Optimization: A vector of decision or design variables belongs to the Pareto optimal set or set of nondominated solutions if there is no other solution that could improve the value of one of the objective functions without deteriorating at least one of the others objective functions. Examples of Pareto solutions are the solutions obtained by optimizing the objective functions individually.

In the case of Pareto optimization, no information is assumed regarding the designer except for his "preference independence." Preference independence describes the situation where lowering the values of the objective function is always better (assuming the problem is one of minimization). The methods in this category attempt to provide a representative approximation of the Pareto optimal set and some of the criteria to evaluate such methods include:

1) how good is the approximation provided by the method of the Pareto optimal set and if it is able to generate a nonconvex Pareto set; that is, a Pareto set represented by a nonconvex curve;
2) how fast the computational effort of its use grows with respect to the number of variables;
3) how easy it is to implement.

Some of the methods that belong to this category are: the weighting method, the noninferior set method and the restriction method (Balachandran *et al.* [15]).

The Pareto optimization in this work is conducted using the weighting method. The weighting method converts the multiobjective problem to a scalar optimization problem, in which the objective function becomes a weighted sum of the individual objective functions. That is

$$\min \sum_{i=1}^{n} w_i f_i(\overline{x}) \quad \text{with} \quad 1 \le i \le n$$

wherein, the w_i's represent the weights and the f_i's represent the individual objective functions. The above problem is a single-objective optimization problem and it is solved using a genetic algorithm. This is a very simple approach that fits the purpose of this investigation. However, the weighting method is not without its drawbacks: it does not uncover solutions in nonconvex regions of the Pareto optimal set; and it finds the Pareto optimal set by solving multiple scalar optimization problems (different set of weights) which may be computationally expensive.

Studies of Pareto optimization using genetic algorithms to obtain the set of nondominated solutions at once have been attempted. The first effort in the use of genetic algorithms in multiobjective optimization problems (Pareto optimization) is due to Shaffer [39]. In his genetic algorithm the population is divided into sub-populations with the fitness of the chromosomes in different sub-populations being evaluated using the different objective functions. Shaffer's approach has the problem that it does not provide a uniform approximation of the Pareto set with the solutions obtained concentrated around the extremes of the nondominated solutions set. A recent genetic algorithm claiming to provide a good approximation of the Pareto optimal set using genetic algorithms is reported by Horn *et al.* [40].

2) Multiattribute Utility Analysis: Pareto optimization is a member of a family of methods based on the measurement of

the values of each objective function and on the knowledge of their relative priority. While this approach may be found useful, as pointed out by Thurston [17], it is limited in two respects:

1) the direct measurement of the objective functions or attributes of the design, does not necessarily reflect the subsequent value or worth to the designer;
2) methods that rely on the concept of relative importance or priority might not accurately quantify attribute tradeoffs.

Attribute tradeoffs refer to the designer's willingness to "pay" for improvement in one attribute at the expense of the other. In contrast to Pareto optimization, MUA concentrates on finding the overall value of the designs; hence, the design with the highest value to the designer can be identified.

The MUA method becomes practical when the so called *preferential* and *utility* independence assumptions are met. Preferencial independence makes reference to situations where the designer always prefers less to more of an attribute (or more to less depending of the attribute) regardless of the level of the other attributes. Utility independence means that the general shape of the utility functions associated with each attribute (to be discussed later) is not altered by levels of the other attributes. Under this conditions, the overall worth of a design $U(\vec{f})$ can be calculated using (8) (see Keeney *et al.* [16])

$$U(\vec{f}) = \frac{1}{K}\left(\{\Phi_{i=1}^{n}[Kk_iU_i(f_i)+1]\}-1\right) \tag{8}$$

wherein

$U(\vec{f})$	overall worth of the set of attributes f_i;
f_i	level of attribute f_i;
$\vec{f}$	set of attributes levels $(f_1, f_2, \cdots f_n)$;
k_i	assessed single attribute scaling constant;
$U_i(f_i)$	assessed single attribute utility function;
K	scaling constant;
n	number of attributes.

If the more restrictive additive independence condition reported by Thurston [17] is satisfied, that is

$$\sum_{i=1}^{n} k_i = 1. \tag{9}$$

It can be shown that (8) reduces to

$$U(\vec{f}) = \sum_{i=1}^{n} k_iU_i(f_i). \tag{10}$$

Equation (10) leaves the designer with two tasks:

1) the identification of the worth of the different levels of each attribute in isolation expressed in the single attribute utility function $U_i(f_i)$;
2) a measure of the tradeoffs the designer is willing to make, in the form of the attribute's scaling constant k_i.

The constants k_i should not be confused with relative importance of attributes or weighting factors.

Points in the single attribute utility functions $U_i(f_i)$ and the attribute's scaling constant k_i can be obtained using the "certainty equivalent" method. An example of the lottery questions used in the certainty equivalent method to determine points in the utility function $U_i(f_i)$ is given in Fig. 4.

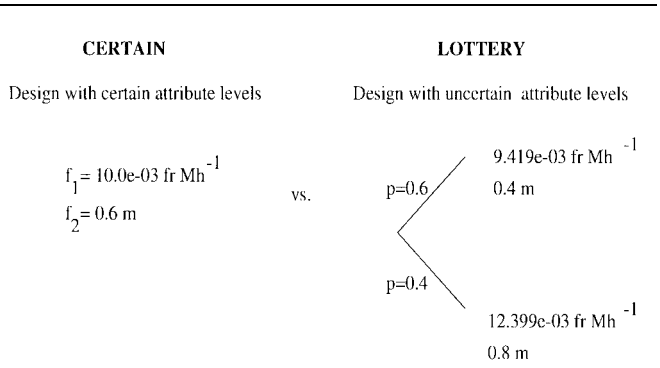

Fig. 4. An example of the lottery questions used in the certainty equivalent method to assess the single attribute utility function $U_i(f_i)$ for failure rate.

The designer is asked to imagine two alternative designs: the "certain" alternative is known with certainty to be some value f, while the "lottery" alternative represents a design alternative in which there is uncertainty as to the attribute level. The lottery in Fig. 4, shows a probability p of 30% that the failure rate (f_1) will be at the estimated best possible level (f_{1b}) and a probability of $(1-p)$ of 70% that failure rate will be at the estimated worst possible value (f_{1w}). When the indifference point is reached, that is, when the designer is equally likely to take the "lottery" or stay with the "certain" alternative, a point in the single attribute utility function, $U_i(f_i) = p$, is obained. The following equations shows the derivation of this result:

$$U_i(f_i) = p \cdot U_i(f_{ib}) + (1-p)\cdot U(f_{iw}) \tag{11}$$
$$U_i(f_i) = p \cdot (1) + (1-p)\cdot (0) \tag{12}$$
$$U_i(f_i) = p. \tag{13}$$

The value of p at which the designer will be indifferent is obtained by iterating through extreme values of p.

The value of k_i is equal to the utility where the attribute f_i is at its best level, f_{ib} and all of the other attributes are at their worst levels; at this point $U(f_{1w}, \cdots f_{ib}, \cdots f_{nw}) = k_i$. The "certain" alternative shown in Fig. 5 represents a design alternative with attribute levels known with certainty, and the lottery represents a design with uncertain attribute levels. The lottery shows a probability p of 60% that the design has the estimated best attribute levels ($f_1 = 9.419\text{e}-03$ fr Mh^{-1}; $f_2 = 0.4$ m) and a probability $(1-p)$ and a probability of 40% that the design will exhibit the estimated worst attribute levels ($f_1 = 12.399-03\text{fr Mh}^{-1}$; $f_2 = 0.8$ m).

The value of k_i is equal to the value of p corresponding to the indifference point; see the following equations for the derivation of this result:

$$U(f_{1w}\cdots f_{ib}\cdots f_{nw}) = p\cdot U(\vec{f_b}) + (1-p)\cdot U(\vec{f_w}) \tag{14}$$
$$U(f_{1w}\cdots f_{ib}\cdots f_{nw}) = p\cdot (1) + (1-p)\cdot (0) \tag{15}$$
$$U(f_{1w}\cdots f_{ib}\cdots f_{nw}) = k_i. \tag{16}$$

Details of the certainty equivalent method can be found in Keeney *et al.* [16].

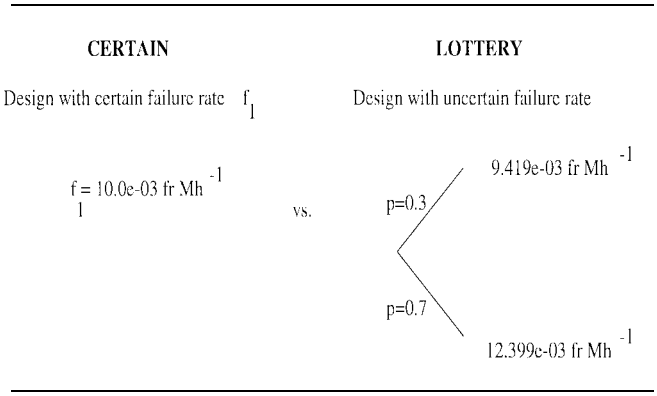

Fig. 5. An example of the lottery questions used in the certainty equivalent method to assess the single attribute scaling constant k for failure rate (k_1).

TABLE II
THERMAL CHARACTERISTICS OF THE HEATED ELEMENTS CONSIDERED IN THE PRESENT CASE STUDY

Element	Height (cm)	q_i (W m^{-2})	B_i (fr Mh^{-1})
1	0.2	200	400
2	0.2	300	400
3	0.2	200	1600
4	0.2	300	1600
5	0.4	200	400
6	0.4	300	400
7	0.4	200	1600
8	0.4	300	1600

IV. CASE STUDY

For the purpose of illustrating and evaluating the present solution methodology, a case study is introduced. With reference to Fig. 1, the case study represents the problem of optimally placing a set of eight heated elements with heat flux and thermal sensitivities as specified in Table II using the solution methodology discussed in the previous section. The optimal placement includes both the minimization of the failure rate of the system (2) and the minimization of the wiring length (3) using an interconnectivity matrix to be specified later.

Using an arrangement considered representative of the set of possible configurations (*15 263 748*), a grid refinement study was first conducted. The grid refinement study included three different nonuniform grids: 110 × 48, 150 × 56, and 186 × 68, and $l_d/h = 4.5$ and 6.0. The description of the grids corresponds to number of nodes in the streamwise and transverse direction, respectively. In all cases, the difference in the prediction of the maximum temperature on each of the heated elements were not significantly affected. The parameter Gr/Re^2 was <1, where $Gr = g\beta(T^{\max} - T_o)\mathrm{w}^3/\nu^2$ is the Grashof number. Therefore, the assumption of negligible natural convection effects is justified.

Throughout the rest of the study (except for the validation run, to be discussed later) the maximum temperatures on the heated elements along the channel were computed using the 110 × 48 grid with $l_d/h = 4.5$. The selected grid has, in the streamwise direction, expansion factors in the interval [1.04, 1.43] and a minimum grid spacing of 0.08. In the transverse direction, the expansion factors are in the interval [1.11, 1.51] and a minimum grid spacing of 0.05. This grid allows the prediction of the maximum temperature of the heated elements within 1% of those obtained using the most refined grid with 75% less CPU time. For the case study, the results of using the two multiobjective optimization strategies under consideration, that is, Pareto optimization and MUA, are presented.

TABLE III
THERMAL CHARACTERISTICS OF THE HEATED ELEMENTS CONSIDERED IN THE VALIDATION RUN

Element	Height (cm)	q_i (W m^{-2})	B_i (fr Mh^{-1})
1	0.2	400	200
2	0.2	400	800
3	0.2	400	2000
4	0.2	400	2000
5	0.2	400	200
6	0.2	400	800
7	0.2	400	2000
8	0.2	400	800

Before presenting and discussing the results associated with these two multiobjective optimization strategies, a thermal placement problem with *known* optimal solutions is first addressed (Validation run).

A. Validation Run

Consider the placement of the heated elements listed in Table III so that the total failure rate of the system (2) is minimized. Observe that the heated elements generate the same heat flux and that the maximum temperature of the heated elements is only a function of their position along the channel. Under these conditions, it can be shown (Queipo *et al.* [14]) that the optimal arrangement requires placing the heated elements in descending order of thermal sensitivity. Hence, optimal sequences are, for example, *34726815*, *74386251*, *43762815*, etc. The total number of possible arrangements is 40 320 (8!), and there are 72 ($3! \times 3! \times 2!$) optimal solutions representing 0.18% of the total solution space.

B. Control Parameters for the Genetic Algorithm

The population size was taken as seven (as in Queipo *et al.* [12]) and the number of generations was specified as nine. Numerical simulations of the genetic algorithm were conducted for a range of crossover rates, mutation rates and scaling factors. The crossover rate and mutation rates considered were between 0.1 and 0.9 with increments of 0.1 (with the restriction of mutation rates lower than crossover rates). The scaling factors were taken between 1.0 and 3.0 with increments of 1.0. The present genetic algorithm exhibited a robust behavior. At the end of nine generations, a significant number of combinations of crossover rate, mutation rate and scaling factor (C, M, S) generated optimal solutions. For example (0.9, 0.4, 1.0), (0.9, 0.2, 1.0), (0.8, 0.4, 1.0), (0.6, 0.3, 1.0), (0.4, 0.1, 1.5), (0.8, 0.4, 1.5), (0.4, 0.1, 2.0), and many others. All the results reported in this section and throughout the study correspond to a crossover rate of 0.9, a mutation rate of 0.4 and a sigma scaling factor equal to 1.0.

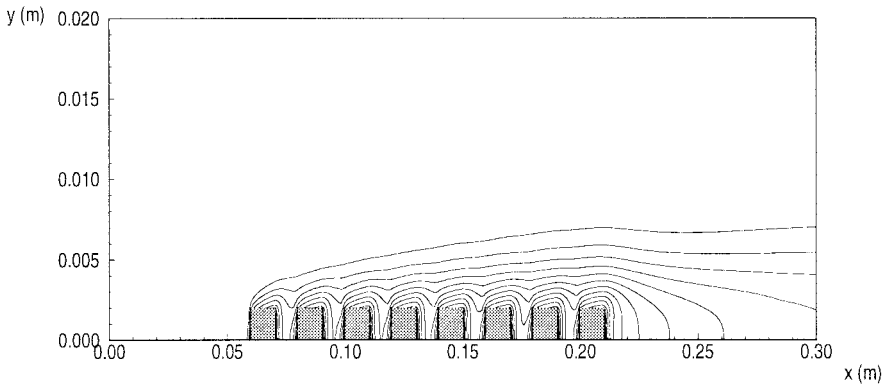

Fig. 6. Temperature isocontours corresponding to the validation run. The figure shows 15 equally spaced contours between 302 and 330 K.

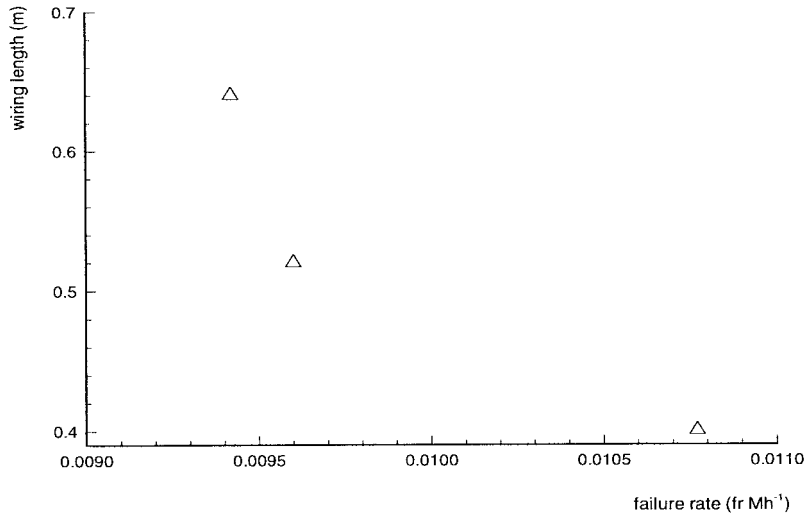

Fig. 7. Solutions uncovered by the genetic algorithm (Pareto optimization).

TABLE IV
TEN BEST ARRANGEMENTS UNCOVERED BY THE CSGA (VALIDATION RUN)

Arragement	f (fr Mh^{-1})	Gen.	Fn. Evals
4 7 3 6 8 2 1 5	*5.643e-03*	*9*	*57*
4 7 3 2 5 6 1 8	5.700e-03	2	19
4 3 7 6 5 2 1 8	5.700e-03	8	53
3 7 4 8 5 6 1 2	5.700e-03	9	58
7 3 4 6 5 2 1 8	5.700e-03	7	47
4 3 7 2 5 6 1 8	5.700e-03	7	51
7 3 4 2 5 6 1 8	5.700e-03	5	37
4 7 3 6 5 8 1 2	5.700e-03	8	56
3 7 4 6 8 2 1 5	*5.643e-03*	*8*	*54*
4 7 3 6 5 2 1 8	5.700e-03	4	30

Fig. 6 shows temperature isocontours corresponding to the Validation run. As expected, the maximum temperatures of the heated elements increase with positions farther downstream of the inflow boundary and the maximum temperature gradients are located near the walls of the heated elements.

Table IV shows the ten best arrangements uncovered by the genetic algorithm. Each entry in the table shows a given arrangement of components, its failure rate, the number of the generation in which it appeared and the corresponding number of objective function evaluations. The best elements correspond to the sequences *47368215* (ninth generation—fifty seven objective function evaluations) and *37468215* (eighth generation—fifty four objective function evaluations) with failure rate of $5.643 - 03$ fr Mh^{-1}. These sequences have the heated elements positioned in decreasing order of thermal sensitivity and are optimal solutions. Note that the expected number of objective function evaluations to randomly find an optimal solution is given by the number of possible arrangements (8!) divided by the number of optimal solutions ($3! \times 3! \times 2!$) and equal to 560. The genetic algorithm found an optimal solution using an order of magnitude fewer objective function evaluations.

V. RESULTS AND DISCUSSION

This section addresses the more complex situation where all the heated elements are different in their heat generation rates or their thermal sensitivities and the optimization criteria include both *thermal* and *nonthermal* optimization criteria. As previously discussed, in the case of multiobjective optimization there is not a general definition of the optimal values and no single best approach for solving these problems. As a result, different philosophies and methodologies, such

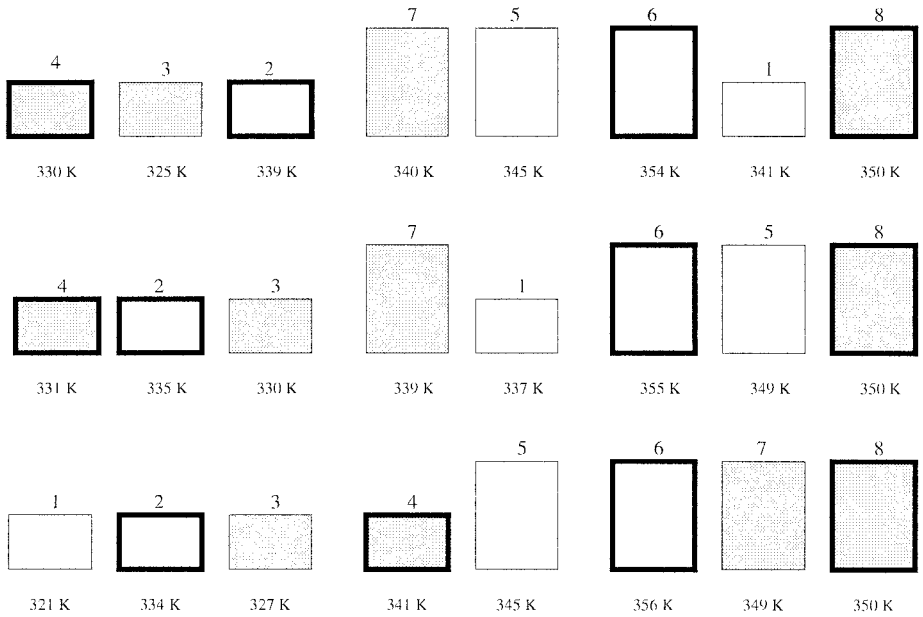

Fig. 8. Best arrangements obtained by the CSGA using Pareto optimization for the cases of (w_λ, w_g): (1.0, 0.0), (0.5, 0.5), and (0.0, 1.0). Top: (1.0, 0.0); 43275618, $f_1 = 9.419\text{e}-03$ fr Mh^{-1} and $f_2 = 0.64$ m. Middle: (0.5, 0.5); 42371658, $f_1 = 9.419\text{e}-03$ fr Mh^{-1} and $f_2 = 0.52$ m. Bottom: (0.0, 1.0); 12345678, $f_1 = 10.770\text{e}-03$ fr Mh^{-1} and $f_2 = 0.4$ m. Maximum temperatures of the heated elements are also shown.

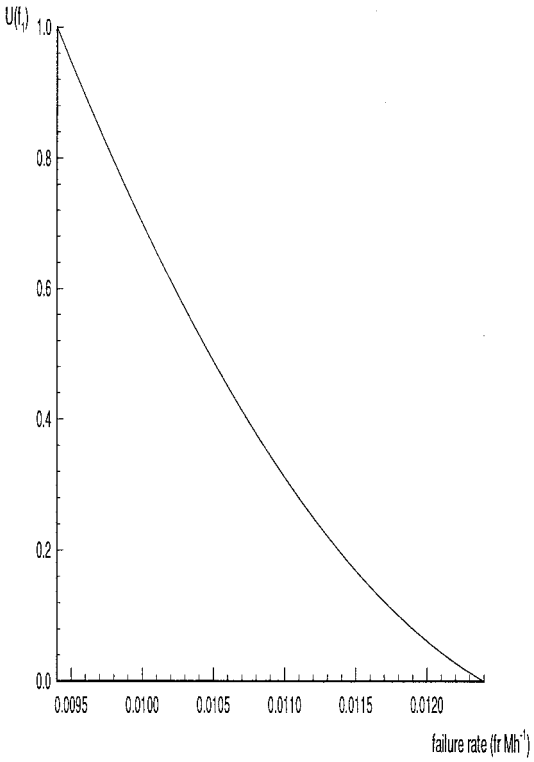

Fig. 9. Single attribute utility function for *failure rate*.

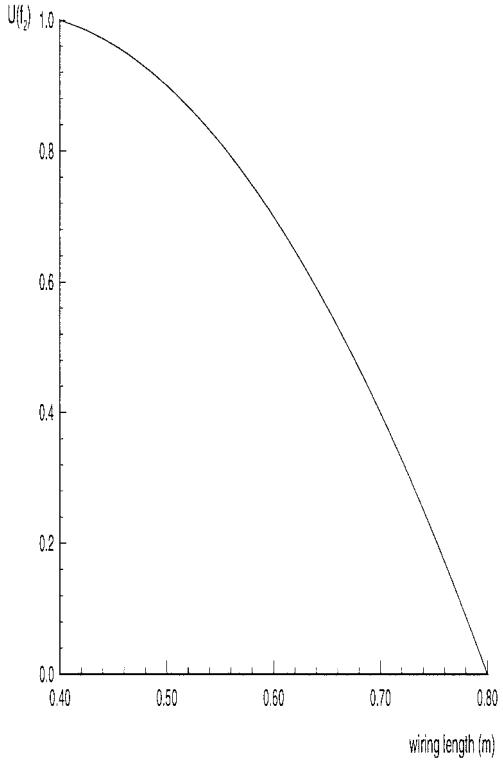

Fig. 10. Single attribute utility function for *wiring length*.

as Pareto optimization and MUA, co-exist for addressing optimization problems with multiple objectives.

The *thermal* and *nonthermal* optimization criteria correspond to the minimization of the failure rate of the system computed using the Arrhenius relation and of the total wiring length according to an interconnectivity matrix. The present interconnectivity requirement is that the heated elements identified with numbers between *1* and *4* inclusive and those identified with numbers between *5* and *8* must be wired among themselves, respectively. The total interconnectivity length and total failure rate of the arrangements of heated elements are denoted by the functions λ (2) and g (3), respectively.

Table II presents a description of the thermal characteristics of the heated elements under consideration. The control parameters of the genetic algorithm adopted were exactly those selected in the Validation run.

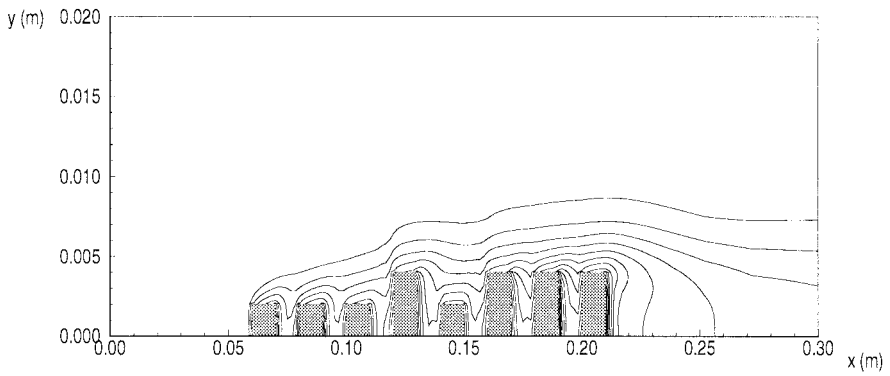

Fig. 11. Temperature isocontours associated with the best arrangement (*42371568*) uncovered by the CSGA. The figure shows 15 equally spaced contours between 302 and 352 K. (MUA).

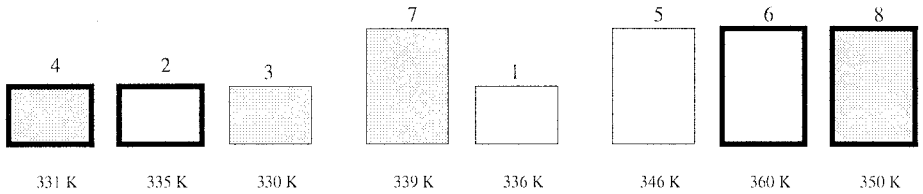

Fig. 12. Maximum temperatures of the heated elements associated with the best arrangement uncovered by the CSGA; $f_1 = 9.725 - 03$ fr Mh^{-1} and $f_2 = 0.52$ m. (MUA).

A. Pareto Optimization

Solutions expected to belong to the Pareto optimal set are calculated using the weighting method (Balachandran *et al.* [15]) which converts the multiobjective problem to a single objective problem, in which the function to be optimized is the weighted sum of the individual objective functions. In this case, the function f to be minimized has the form

$$f = w_\lambda * \lambda_{\text{total}} + w_g * (C_o g) \tag{17}$$

where C_o represents a scaling factor, calculated for each generation in order to render the average contribution of the interconnectivity term in the sum comparable in magnitude to the average contribution due to the total failure rate. The coefficients w_λ and w_g are weighting factors representing the relative importance of the optimization criteria, with $w_\lambda + w_g = 1$. In this work, three points in the Pareto optimal set (including the extremes of the set and a situation where the optimization criteria are considered to be equally important) are sought (w_λ, w_g): (1.0, 0.0), (0.5, 0.5), and (0.0, 1.0).

The failure rate and interconnectivity length associated with the three Pareto optimal solutions are plotted in Fig. 7. The solution corresponding to weighting factors (1.0, 0.0) has a failure rate of 9.419 fr Mh^{-1} and an interconnectivy length of 0.64 m. This solution was found after five generations (thirty one objective function evaluations) and corresponds to a situation where the minimization of the failure rate is the sole optimization criterion. A solution corresponding to the other extreme of the Pareto optimal set; that is, the situation where the minimization of the wiring length is the only optimization criterion ($w_\lambda = 0$ and $w_g = 1.0$) was selected by inspection of the interconnectivity requirement. The optimal solution selected for this case was the sequence *12345678* with a failure rate of 10.770 fr Mh^{-1} and an optimal wiring length of 0.4 m. The Pareto optimal solution associated with the situation with equal weighting factors was obtained after nine generations (sixty six objective function evaluations) and corresponds to the sequence *42371658*. The aforementioned sequence has a failure rate of 9.600 fr Mh^{-1} and an interconnectivity length of 0.52 m. Note that the Pareto optimal solutions under consideration are in fact nondominated solutions (see Fig. 8), with their failure rate and interconnectivity length varying by up to 14 and 60%, respectively.

TABLE V
TEN BEST ARRANGEMENTS UNCOVERED BY THE CSGA (MULTIATTRIBUTE UTILITY ANALYSIS)

Arragement	Utility	Gen.	Fn. Evals
4 2 3 7 5 6 1 8	7.8583e-01	1	11
4 2 3 7 6 5 1 8	7.1768e-01	4	35
3 2 4 7 5 6 1 8	7.2541e-01	6	48
2 3 4 7 5 6 1 8	7.0141e-01	0	7
4 2 3 5 7 6 1 8	6.8448e-01	5	39
4 2 3 6 1 7 5 8	8.1152e-01	8	63
4 2 3 1 5 6 7 8	7.6526e-01	6	47
3 4 2 8 5 6 1 7	6.9352e-01	1	13
4 2 3 6 5 7 1 8	7.5229e-01	4	32
4 2 3 7 1 5 6 8	*8.4586e-01*	9	*65*

B. Multiattribute Utility Analysis

This section discusses the solution of the case study using the single attribute utility functions for failure rate (f_1) and wiring length (f_2) shown in Figs. 9 and 10, respectively. Figs. 9 and 10 corresponds to quadratic polynomials that interpolate the points [f_1, $U(f_1)$]: (9.4e $-$ 03 fr Mh^{-1}, 1.0).

(10.0e − 03 fr Mh^{-1}, 0.7), (12.4e − 03 fr Mh^{-1}, 0.0); and the points [f_2, $U(f_2)$]: (0.4 m, 1.0), (0.6 m, 0.7), (0.8 m, 0.0), respectively.

The scaling factors reflecting acceptable tradeoffs between attributes, are given as $k_1 = 0.6$ (failure rate) and $k_2 = 0.4$ (wiring length). Both, the utility functions and the scaling factors are assumed to have been obtained with the participation of the designer and the certainty equivalent method discussed in a previous section. The function to be maximized is given by (10) with the aforementioned utility functions and scaling factors.

The ten best arrangements obtained when using the MUA approach are shown in Table V. The best arrangement corresponds to the sequence *42371568* with a failure rate and wiring length of 9.725e−03 fr Mh^{-1} and 0.52 m, respectively. The best arrangement was found after nine generations and 65 function evaluations.

The temperature isocontours as well the maximum temperature on each of the heated elements corresponding to the sequence *42371568* are shown in Figs. 11 and 12, respectively.

Note that this approach provides the \"best\" solution with a single coupled execution of the fluid and heat transfer solver and the genetic algorithm provided the utility functions (U_i) and the scalar constants (k_i) are available. In addition, this approach could be used to identify the "best" solution among the Pareto optimal solutions found (those obtained in the previous section) by computing the utility value of each of the Pareto optimal solutions and selecting the solution with highest utility value.

VI. Conclusion

A model for the problem of optimal placement of electronic components on printed wiring boards subject to *thermal* and *nonthermal* optimization criteria has been formulated and solved using a methodology based on three components:

1) a fluid and heat transfer solver for the prediction of the maximum temperature of the heated elements;
2) a multiobjective optimization strategy for the scalarization of the vector of design objectives;
3) a genetic algorithm for the search of optimal or near optimal solutions.

The multiobjective optimization strategy embedded in the solution methodology is flexible enough to account for two extreme situations (no knowledge/knowledge) regarding the knowledge of the preference structure of the designer by using Pareto optimization and MUA.

The solution methodology shows promise as an effective and efficient tool for providing optimal or near-optimal solutions for electronic component placement problems where both thermal and nonthermal optimization criteria are of interest under rather general conditions regarding component geometries, heat generation rates and thermal sensitivities.

Acknowledgment

The authors would like to thank the IBM Corporation for providing the RISC 6000 workstation, which performed the calculations for the project.

References

[1] L. Moresco, "Electronic system packaging: The search for manufacturing the optimum in a sea of constraints," in *7th IEEE/CHMT Int. Electron. Manufact. Technol. Symp.*, 1989, pp. 149–164.
[2] J. Weiss, P. Fortner, B. Pearson, K. Watson, and T. Monroe, "Modeling air flow in electronic packages," *Mech. Eng.*, pp. 56–58, Sept. 1989.
[3] H. Wessely, O. Fritz, M. Horn, P. Klimke, W. Koschnick, and K. Schmidt, "Electronic packaging in the 1990's: The perspective from Europe," *IEEE Trans. Comp., Hybrids, Manufact. Technol.*, vol. 14, pp. 272–284, June 1991.
[4] D. Dancer and M. Pecht, "Component placement optimization for convectively cooled electronics," *IEEE Trans. Syst., Man, Cybern.*, vol. 18, pp. 199–205, 1989.
[5] M. Osterman and M. Pecht, "Component placement for reliability on conductively cooled printed wired boards," *J. Electron. Packag.*, vol. 111, pp. 149–155, 1989.
[6] R. Eliasi, T. Elperin, and A. Bar-Cohen, "Monte Carlo thermal optimization of populated printed circuit board," *IEEE Trans. Comp., Hybrids, Manufact. Technol.*, vol. 13, pp. 953–960, Dec. 1990.
[7] S. Kirkpatrick, C. Gelatt, and M. Vecchi, "Optimization by simmulated annealing," *Science*, vol. 220, pp. 671–680, 1983.
[8] A. Dunlop and B. Kernighan, "A procedure for placement of standard-cell VLSI circuits," *IEEE Trans. Computer-Aided Design*, vol. CAD-4, pp. 92–98, Jan. 1985.
[9] K. Shahookar and P. Mazumder, "A genetic approach to standard cell placement using meta-genetic parameter optimization," *IEEE Trans. Computer-Aided Design*, vol. CAD-9, pp. 500–511, May 1990.
[10] M. Osterman and M. Pecht, "Placement for reliability and routability of convectively cooled PWB's," *IEEE Trans. Computer-Aided Design*, vol. 9, pp. 734–744, July 1990.
[11] M. Pecht, M. Palmer, W. Schenke, and R. Porter, "An investigation into PWB component-placement tradeoffs," *IEEE Trans. Rel.*, vol. R-36, Dec. 1987.
[12] N. Queipo, R. Devarakonda, and J. A. C. Humphrey, "Genetic algorithms for thermosciences research: Application to the optimized cooling of electronic components," *Int. J. Heat Mass Transf.*, vol. 37, no. 6, pp. 893–908, 1994.
[13] N. Queipo, J. A. C. Humphrey, and A. Ortega, "Optimal placement of convectively and conductively cooled electronic components using genetic algorithms," in *Proc. Symp. Honor Chancellor Chang-Lin Tien*, Univ. California, Berkeley, 1995, pp. 453–464.
[14] N. Queipo, "On the optimal placement of heat sources in an enclosure based on adaptive search and machine learning," Ph.D. dissertation, Univ. California, Berkeley, 1995.
[15] M. Balanchandran and J. Gero, "A comparison of three methods for generating the Pareto optimal set," *Eng. Optim.*, vol. 7, pp. 319–336, 1984.
[16] R. Keeney and H. Raiffa, *Decision with Multiple Objectives.* Cambridge, U.K.: Cambridge Univ. Press, 1993.
[17] D. Thurston, "A formal method for subjective design evaluation with multiple attributes," *Res. Eng. Design*, vol. 3, pp. 105–122, 1991.
[18] K. Wong, "What is wrong with the existing reliability predictions methods?," *Qual. Rel. Eng. Int.*, vol. 6, pp. 251–257, 1990.
[19] H. Blanks, "Arrhenius and the temperature dependence of nonconstant failure rate," *Qual. Rel. Eng. Int.*, vol. 6, pp. 259–265, 1990.
[20] K. De Jong, "Adaptive system design: A genetic approach," *IEEE Trans. Syst., Man Cybern.*, vol. SMC-10, pp. 566–574, Sept. 1980.
[21] D. Jang, R. Jetli and S. Acharya, "Comparison of the PISO, SIMPLER, and SIMPLEC algorithms for the treatment of the pressure-velocity coupling in steady flow problems," *Numer. Heat Transf.*, vol. 10, pp. 209–228, 1986.
[22] R. Sani and P. Gresho, "Résumé and remarks on the open boundary condition minisymposium," *Int. J. Numer. Meth. Fluids*, vol. 18, pp. 983–1008, 1994.
[23] E. Blosh, W. Shyy, and R. Smith, "The role of mass conservation in pressure-based algorithms," *Numer. Heat Transf*, vol. 24, pp. 415–429, 1993.
[24] S. Kim, "A numerical analysis of convective heat transfer in channels simulating electronic components," Ph.D. dissertation, Texas A&M Univ., College Station, 1993.
[25] T. Hayase, J. A. C. Humphrey, and R. Greif, "ROTFLO2 (A general computer program for three-dimensional laminar flow and heat transfer in axisymmetrically confined region): Mini-manual," Mech. Eng. Dept., Univ. California, Berkeley, Tech. Rep. FM-90-1, 1990.
[26] S. Patankar, *Numerical Heat Transfer and Fluid Flow.* Washington, DC: Hemisphere, 1980.
[27] T. Hayase, J. A. C. Humphrey, and R. Greif, "A consistently formulated QUICK scheme for fast and stable convergence using finite-volume

iterative calculation procedures," *J. Comput. Phys.*, pp. 108–118, Jan. 1992.
[28] S. Patankar and D. Spalding, "A calculation procedure for heat, mass and momentum transfer in three-dimensional parabolic flows," *Int. J. Heat Mass Transf.*, vol. 15, pp. 1787 and 1807, 1972.
[29] J. Van Doormaal and G. Raithby, "Enhancements of the SIMPLE method for predicting incompressible fluid flows," *Numer. Heat Transf.*, vol. 7, pp. 147–163, 1984.
[30] U. Ghia, K. Ghia, and C. Shin, "High-resolutions for incompressible flow using the Navier–Stokes equations and a multigrid method," *J. Comput. Phys.*, vol. 48, pp. 387–411, 1982.
[31] D. Gartling, "A test problem for outflow boundary conditions—Flow over a backward facing step," *Int. J. Numer. Meth. Fluids*, vol. 11, pp. 953–967, 1990.
[32] A. Runchal, "ANSWER: A benchmark study for backward facing step," *Benchmark Prob. Heat Trans. Codes ASME*, vol. HTD-222, pp. 13–19, 1992.
[33] M. Dainese, *Simulation D'Écoulements de Fluide Incompressible en Géométrie Complexe: Contribution á L'Étude des Schémas de Discrétization et D'Algorithmes Semi-implicites*, Ph.D. thesis, L'École Nationale Supérieure de L'Aéronautique et de L'Espace, Toulouse, France, 1994.
[34] M. Peric, "A finite volume method for the prediction of three-dimensional numerical fluid flow in complex ducts," Ph.D. thesis, Imperial College, London, U.K., 1985.
[35] N. Schraudolph and J. Grefenstette, "A user's guide to GAucsd 1.4," Available via anonymous ftp from cs.ucsd.edu (132.239.51.3) in the pub/GAucsd directory, 1992.
[36] W. Press, B. Flannery, S. Teukolsky, and W. Vetterling, *Numerical Recipes—The Art of Scientific Computing.* Cambridge, U.K.: Cambridge Univ. Press, 1986, p. 197.
[37] J. Holland, *Adaptation in Natural and Artificial Systems.* Cambridge, MA: MIT Press, 1975.
[38] D. Goldberg, *Genetic Algorithms in Search, Optimization and Machine Learning.* Reading, MA: Addison-Wesley, 1989.
[39] J. Shaffer, "Multiobjective optimization with vector evaluated genetic algorithms," in *Proc. 1st Int. Conf. Genetic Algorithms*, 1985, pp. 93–100.
[40] J. Horn and N. Nafpliotis, "Multiobjective optimization using niched pareto genetic algorithms," Univ. Illinois, Urbana–Champaign, Rep. 93005.

Nestor V. Queipo received the B.Sc. degree in civil engineering and the M.Sc. degree in computer science from the University of Zulia, Venezuela, and the Ph.D. degree in mechanical engineering from the University of California at Berkeley.

He was a member of the faculty of the Aerospace and Mechanical Engineering Department, University of Arizona, Tucson, and is currently Associate Professor and Director of the Applied Computing Institute, University of Zulia. His research interests include prediction of transport phenomena, analysis of complex data, surrogate modeling and optimal design of complex systems, and nonlinear process control.

Joseph A. C. Humphrey received the Ph.D. and D.Sc. Eng. degrees from the Imperial College of Science, Technology, and Medicine, London University, London, U.K., in 1977 and 1997, respectively.

He became Dean and Professor of Mechanical Engineering at Bucknell University, Lewisburg, PA, in August 1997. From 1977 to 1995, he was on the faculty of the Department of Mechanical Engineering, University of California, Berkeley, and from 1995 to 1997, he was Head of Aerospace and Mechanical Engineering at the University of Arizona, Tucson. His teaching and research interests are in fluid mechanics and transport phenomena, with emphasis on the application of experimental and computational methodologies to problems ranging from multiphase flows through complex geometries to microsensing in arthropods.

Dr. Humphrey is an active member of several major engineering societies, editorial, and industrial boards, and the recipient of various awards and honorary professorships, including Fellow of the ASME and Fulbright Fellow.

Alfonso Ortega (M'96) received the B.S. degree from the Univeristy of Texas, El Paso, in 1976 and the M.S. and Ph.D. degrees from Stanford University, Stanford, CA, in 1978 and 1986, respectively, all in mechanical engineering.

He was a Member of the Technical Staff at Sandia National Laboratories, Albuquerque, NM, in the Fluid and Thermal Sciences Division, from 1978 to 1981, and in the Geothermal Research Division, from 1986 to 1988. In 1988, he joined the faculty of the Department of Aerospace and Mechanical Engineering, University of Arizona, Tucson, where he is currently Associate Professor. His research is in the area of experimental and numerical convective heat transfer in complex forced and buoyant flows, especially those arising in air cooling of electronics and cooling of turbomachinery. He established the AME Heat Transfer Laboratory at the University of Arizona in 1988 and is a member of the University of Arizona Center for Electronics Packaging Research. He is the author of numerous technical papers and book chapters on air cooling of electronics, and is a frequent lecturer on the subject, both in the United States and abroad. He is currently Associate Technical Editor of the *ASME Journal of Electronic Packaging*. He currently holds positions as Guest Researcher in the Semiconductor Electronics Division at the National Institute of Standards and Technology, Gaitherburg, MD and Visiting Guest Scientist at the Burger Center for Fluid Mechanics at the Technical University of Delft, Delft, The Netherlands.

Dr. Ortega has served as Chairman of the ASME Heat Transfer Division K-16 Committee on Heat Transfer in Electronic Equipment from 1993 to 1997, General Chairman of the 1994 IEEE SEMITHERM Conference, and General Chairman of the 1994 ASME-IEEE ITHERM Conference. In 1990, he was named a National Science Foundation Presidential Young Investigator.